EUROPEAN FUSION DEVELOPMENT AGREEMENT

EFDA–JET–CP(01)02-02

G.L. Jackson, M. Murakami, D.R. Baker, R. Budny, M. Charlet,
M.R. deBaar, P. Dumortier, T.E. Evans, R.J. Groebner, N.C. Hawkes,
D. Hillis, L.C. Ingesson, E. Joffrin, H.R. Koslowski, K.D. Lawson,
G. Maddison, G.R. McKee, A.M. Messiaen, P. Monier-Garbet, M.F.F. Nave,
J. Ongena, J. Rapp, F. Sartori, G.M. Staebler, M. Stamp, J.D. Strachan,
M. Tokar, B. Unterberg, M. von Hellerman, M.R. Wade
and JET EFDA Contributors

Comparison of L-Mode Regimes with Enhanced Confinement by Impurity Seeding in JET and DIII-D

Comparison of L-Mode Regimes with Enhanced Confinement by Impurity Seeding in JET and DIII-D

G.L. Jackson[1], M. Murakami[2], D.R. Baker[1], R. Budny[3], M. Charlet[4], M.R. deBaar[5], P. Dumortier[6], T.E. Evans[1], R.J. Groebner[1], N.C. Hawkes[4], D. Hillis[2], L.C. Ingesson[5], E. Joffrin[4], H.R. Koslowski[7], K.D. Lawson[4], G. Maddison[4], G.R. McKee[8], A.M. Messiaen[6], P. Monier-Garbet[9], M.F.F. Nave[10], J. Ongena[6], J. Rapp[7], F. Sartori[4], G.M. Staebler[1], M. Stamp[4], J.D. Strachan[4], M. Tokar[7], B. Unterberg[7], M. von Hellerman[5], M.R. Wade[2]
and JET EFDA Contributors*

[1]*DIII-D National Fusion Facility, San Diego, California, USA*
[2]*ORNL, Oak Ridge, Tennessee, USA*
[3]*Princeton Plasma Physics Laboratory, Princeton, New Jersey*
[4]*Euratom/UKAEA Fusion Association Culham, United Kingdom*
[5]*FOM Institut voor Plasmafysica, Nieuwegein, Netherlands*
[6]*ERM, Brussels, Belgium*
[7]*IPP-Forschungszentrum, Jülich, Germany*
[8]*University of Wisconsin, Madison, Wisconsin, USA*
[9]*CEA Cadarache, France*
[10]*Associação EURATOM/IST, Lisboa, Portugal*
**See appendix of the paper by J.Pamela "Overview of recent JET results", Proceedings of the IAEA conference on Fusion Energy, Sorrento 2000*

Preprint of Paper to be submitted for publication in Proceedings of the EPS Conference,
(Madeira, Portugal 18-22 June 2001)

The use of non-intrinsic impurities in tokamaks can reduce peak heat fluxes to divertor components by reducing power flow across the last closed flux surface, which is desirable for fusion reactors. This reduced heat flow can also allow the discharge to remain below the L-H power threshold, further reducing transient heat pulses, i.e. ELMS, to plasma facing surfaces. An additional benefit of impurity seeding is that, under some conditions, enhanced confinement is also observed [1,2]. Neon seeding has been injected into JET and DIII-D discharges, increasing confinement up to $H_{97Y} = 1.1$, i.e. equivalent to ELMing H-mode, while maintaining an L-mode edge. The purpose of this work is to examine the similarities and differences in such discharges in both tokamaks, providing size scaling and leading to an understanding of the underlying physical mechanisms.

The temporal evolution of JET and DIII-D neon seeded L-mode discharges is quite similar, and is depicted in Fig.1. Neon injection is applied during the current ramp and q_{95} reaches ~ 4.1 (JET) and 3.7 (DIII-D) at current flattop (Fig.1(e)). Both tokamaks exhibit a doubling of the core ion temperature (Fig.1(a)) when compared to reference (no neon) discharges. In both devices, the radiated power fraction increases to 0.5 or more after the neon pulse (Fig.1(b)) and confinement is at or above the H_{97y} ELMing H-mode value (Fig.1(c)). The confinement improvement in JET relative to a baseline discharge is not as dramatic as in DIII-D because the JET reference discharge had an L-H transition at 4.45s, while the DIII-D reference discharge remained in L-mode. This difference is due to the lower H-mode power threshold in JET with the $\nabla B \times B$ drift direction towards the X-point while the drift is opposite in DIII-D. Even though Z_{eff} is higher with neon seeding, the measured neutron rate in both machines increases with neon seeding (Fig.1(d)), although the increase is not as large in JET when comparing to a reference ELMing H-mode. However, thermal neutrons, calculated by the TRANSP code (not shown), showed a dramatic increase in both devices when compared to their reference discharge: up to a factor of 3 in JET and 18 in DIIID.

Profiles of the discharges in Fig.1 are shown in Fig.2 during times when effects of neon seeding were well established: 4.8s (JET) and 1.16s (DIII-D). For the neon seeded discharges, there is an increase in the ion temperature gradient, $-dT_i/d\rho$, at $\rho \sim 0.6$ (DIII-D) and ~ 0.35 (JET). This occurs in the region where χ_i is decreasing rapidly in JET [Fig. 2(b)], although χ_i is already low in DIII-D. Thermal diffusivities are calculated by the TRANSP code. Within the region of higher temperature gradient, described above, plasma thermal pressure, $n_eT_e + \sum n_iT_i$ (Fig.2(d)), is generally higher than the reference discharge, consistent with the lower transport in the neon seeded discharges.

The temporal aspects of JET and DIII-D impurity seeded L-mode discharges are similar, suggesting that the underlying physical mechanisms are also the same. DIIID discharges show a reduction of density fluctuations, measured by Beam Emission Spectroscopy (BES) and this reduction is most pronounced in the region $\rho \sim 0.6–0.7$ [3]. The GyroKinetic Simulation (GKS) code [4] shows that the growth rates of microturbulence in the wavelength range of ITG modes is significantly reduced in DIII-D in this region. This reduction is produced by **E×B** shear stabilization, shown in Fig.3(a), where the shearing rate is greater than the maximum growth rate, γ_{max} over most of the

profile, including the region where density fluctuations are reduced [5]. In the reference discharge (Fig. 3(b)), the **E**×**B** shearing rate is less than γ_{max} for $\rho > \sim 0.6$, and shear stabilization would not be expected in this region. Note that the regions where γ_{max} is not displayed are where the GKS code could not calculate a growth rate.

GKS analysis of JET discharges also predicts a stabilizing effect in the growth rates of microturbulence with the introduction of neon, shown in Fig.4(a). Because no poloidal velocity measurements are presently available in JET, neoclassical estimates of the poloidal rotation velocity are used to estimate the **E**×**B** shearing rate. Since the reference case was an H-mode discharge, stable to ITG modes, this reference discharge is not shown. For the neon seeded case, GKS calculations show that the growth rates are reduced to below the **E**×**B** shearing rate indicating that low k microturbulence for $\rho \lesssim 0.4$ is at least marginally stable. The frequency (Fig.4(b)) is in the ion diamagnetic drift direction in the core of the plasma. However, for $\rho > 0.55$, this frequency changes to the electron diamagnetic drift direction. The range of wavenumbers, k, is consistent with Trapped Electron (TE) modes producing the maximum turbulent growth rates in this region.

As shown in Fig.1, the neutron rate is higher in both devices with the introduction of neon, even though Z_{eff} has also increased. At the times shown in Fig. 2, $\overline{Z_{eff}}$ is 3.2 (DIII-D) and 4.5 (JET). The increase in the neutron rate is consistent with higher core temperatures in the neon cases (Fig.1) and hollow Z_{eff} profiles in both devices. To date, no experiments have been performed to optimize the use of impurities, i.e. to minimize the amount of injected impurities while maintaining improved confinement and the higher **E**×**B** shearing rate shown in Fig. 3.

Impurity seeded L-mode discharges in both JET and DIII-D are limited by MHD activity. In DIII-D m/n=3/2 neoclassical tearing modes (NTM), often triggered by sawteeth, limit the duration of the enhanced performance phase [6]. In JET, early tearing modes (not neoclassical) near the time of neon injection can severely limit performance. In addition, the lower L-H power threshold can produce edge MHD (ELMs) which is also detrimental. In other JET discharges, e.g. Fig.1, higher stored energy and neutron rates may be clamped by the onset of fishbones and sawteeth. In both devices, MHD avoidance is a crucial next step for extending the duration of these types of discharges and evaluating their efficacy. For neon seeded L-mode discharges, ECCD suppression of the m/n=3/2 NTMs has been proposed in DIII-D and Lower Hybrid Current Drive (LHCD) to suppress sawteeth has had some success in JET.

In conclusion, neon seeded discharges with an L-mode edge and confinement equivalent to ELMy H-mode have been achieved in both DIII-D and JET. The temporal evolution of these discharges is similar in both devices. When compared to reference (unseeded) discharges, a region of higher ion temperature is observed, up to a factor of 2 in the center. Higher plasma pressure extends from the core to $\rho \sim 0.6$ in DIII-D and $\rho \sim 0.35$ in JET. The smaller region in JET is one of the differences between these two tokamaks. Whether this is due to differences in operation or is a fundamental difference has not been established, although we note that trapped electron mode turbulence, not stabilized by **E**×**B** shear, is the dominant mode in JET at larger radii, a feature not observed in DIII-D

In both devices, **E×B** shear stabilization of low k (ITG) modes appears to be the physical mechanism leading to lower thermal diffusivities and higher confinement. BES measurements in DIII-D show a reduction in density fluctuations in the wavelength range where such microturbulence is expected. Although such measurements are not available in JET, **E×B** shear stabilization in the region $\tilde{\rho} <$ 0.35 can account for the lower diffusivity and higher ion temperatures. A model which is consistent with these observations is that impurity seeding acts synergistically to reduce low k ion turbulence (ITG modes). Initially the introduction of neon acts as a trigger to decrease the growth rate of the turbulence by increasing the impurity concentration (mass stabilization). This reduction of turbulence leads to lower transport and higher **E×B** shear producing additional stabilization and creating a positive feedback loop.

Future work will be directed at extending the duration of these neon seeded discharges by reducing MHD, using tools such as ECCD and LHCD.

ACKNOWLEDGEMENT

Work partially supported by U.S. Department of Energy under Contracts DE-AC03-99ER54463, DE-AC05-00OR22725, and DE-AC02-76CH03073, and Grant DE-FG03-96ER54373.

REFERENCES

[1]. J. Ongena, A.M. Messiaen, B. Unterberg, et al., Plasma Phys. Control Fusion, **41**, A379 (1999).

[2]. M. Murakami, G.R. McKee, G.L. Jackson, Nucl. Fusion **41**, No. 3, 317–323 (2000).

[3]. G.R. McKee, M. Murakami, J.A. Boedo, et al., Phys. Plasmas **7**, 1870 (2000).

[4]. R.E. Waltz, and R.L. Miller, Phys. Plasmas **6**,4625 (1999).

[5]. K.H. Burrell, Phys. Plasmas **4**, 1499 (1997).

[6]. G.L. Jackson, M. Murakami, G.R. McKee , accepted for publication, Nucl. Fus. (2001).

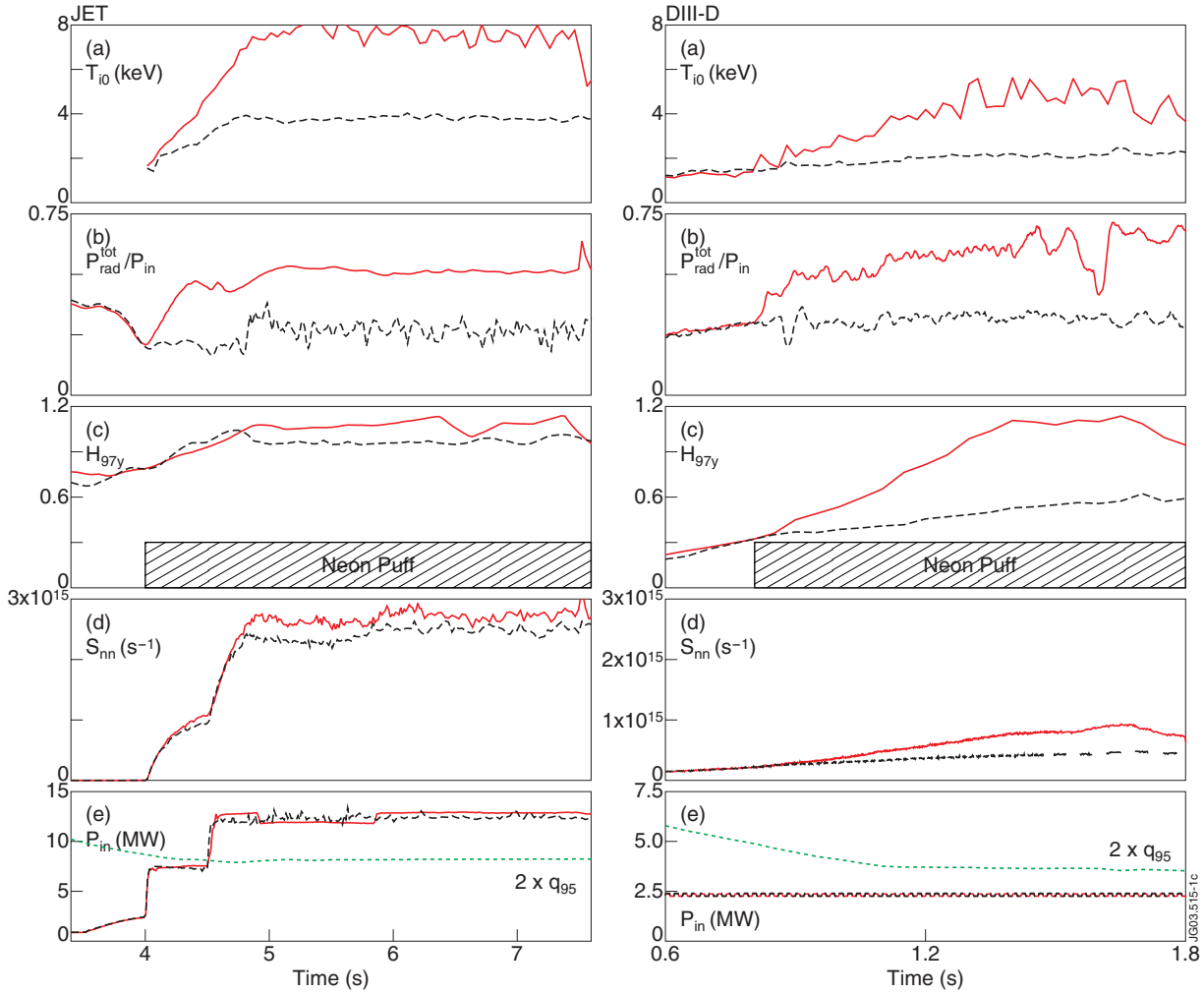

Figure 1: Temporal evolution of JET (left panels) and DIII-D (right panels) neon seeded discharges (Pulse Nos: 53154 and 98775). Reference discharges are also shown (dotted lines, Pulse Nos: 53156 and 98777). Plotted are: $T_i(0)$ (a), radiated power fraction (b), H_{97y} confinement enhancement factor (c), total measured neutron rate (d), and input power (e). Safety factor, q_{95}, is also shown in (e) as dotted lines. Ordinate scales are the same for both DIII-D and JET to allow a direct comparison.

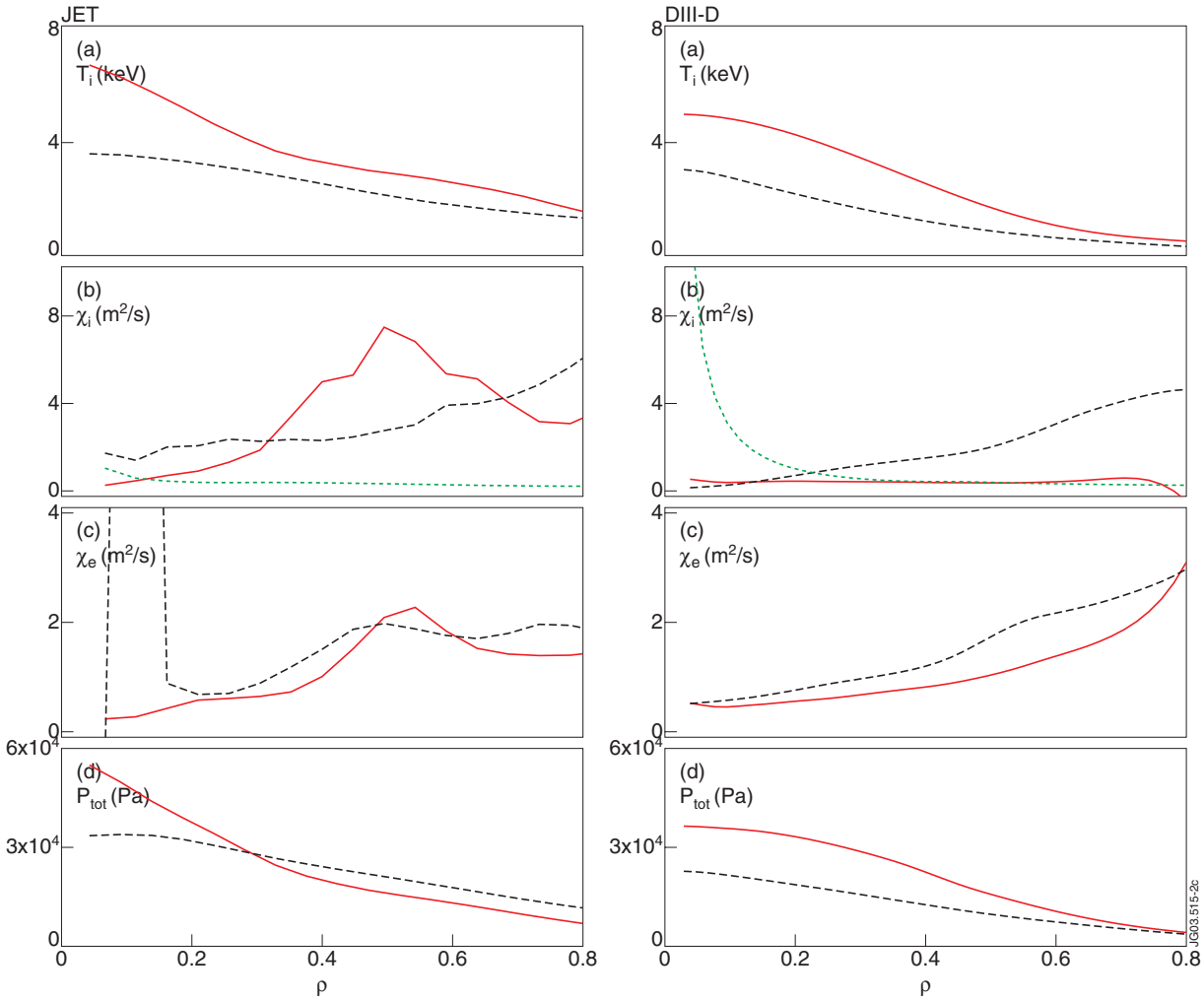

Figure 2: Profiles of (a) T_i, (b) χ_i, (c) χ_e, and (d) plasma thermal pressure for both JET (left panels) and DIII-D (right panels) at 4.8s (JET) and 1.16s (DIII-D). Ion neoclassical diffusivity is shown as a dotted line (b). Reference discharges (no neon) are shown as dashed lines. Discharges are the same as those in Fig. 1.

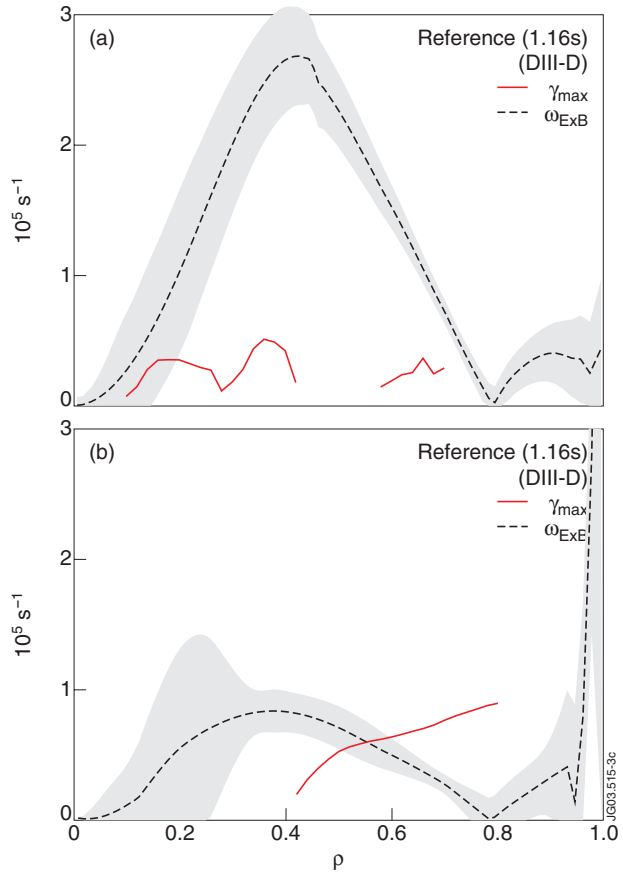

Figure 3: Maximum growth rates and E×B shearing rates for DIII-D discharges with (a) and without (b) neon seeding at 1.16s. Discharges are the same as in Figs. 1 and 2.

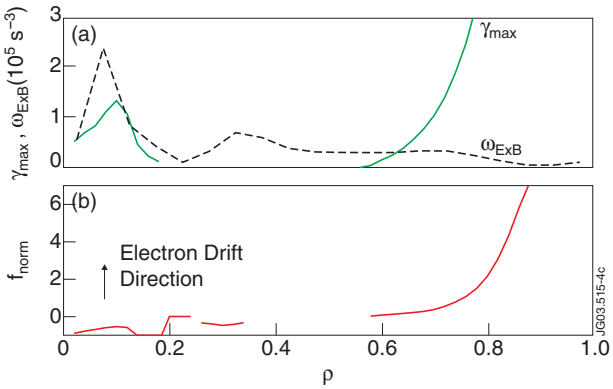

Figure 4: Maximum growth rate and calculated E×B shearing rate for JET Pulse No: 53154 with neon seeding (a). Normalized frequency (b) indicates the γ_{max} is in the ion diamagnetic drift direction for $\rho < 0.4$ and the electron diamagnetic drift direction for $\rho > 0.6$.